Aquat. Living Resour. 2023, 36, 20

https://doi.org/10.1051/alr/2023015

Aquatic Living Resources
Available online at:
www.alr-journal.org

RESEARCH ARTICLE OPEN ACCESS

Spatiotemporal structure of narrow-barred Spanish mackerel (*Scomberomorus commerson*) from the Red Sea and western Indian Ocean based on otolith micro-chemistry

Mohamed A. Sougueh[1,2], Maylis Labonne[3], Abdourahman Daher[1], Ahmed Ali[1] and David M. Kaplan[2]

[1] Marine Biology Laboratory Life Sciences Institute, Center of Study and Research of Djibouti, Route de l'Aéroport, BP 246, Djibouti
[2] MARBEC, Univ. Montpellier, CNRS, Ifremer, IRD, Avenue Jean Monnet, CS 30171, 34203, Sète
[3] MARBEC Univ. Montpellier, CNRS, Ifremer, IRD, Place Eugène Bataillon-Bat 24 CC093 34095, Montpellier, France

Received 4 November 2021 / Accepted 22 May 2023

Handling Editor: Catarina Vinagre

Abstract – Though the narrow-barred Spanish mackerel (*Scomberomorus commerson*) is considered to be migratory, the species is nevertheless thought to be locally overexploited in the northwest Indian Ocean. At the regional level, this local depletion is a major concern for food security. As the population structure and connectivity between sub-populations are poorly understood for this species, we examined the spatio-temporal dynamics of narrow-barred Spanish mackerel via elemental concentrations (P, Mg, Sr and Ba) along otolith transects using LA-ICPMS for samples from 6 sites: Egypt, Djibouti North and South, Somalia, Mozambique and South Africa. For homogeneous size class samples (70–90 cm), otolith chemical signatures immediately preceding capture were used to accurately group individuals sharing a spatial proximity and/or season of capture. Notable differences in otolith edge signatures were found among individuals from north and south of the equator and contrasting cluster compositions from nearby sites in the Gulf of Aden of individuals captured in summer versus winter. Otolith core chemistry identified two spawning chemical compositions. The first common composition was characterized by relatively high concentrations of Sr and lower concentrations of P, Ba and Mg. The second less common spawning chemical composition was particularly rich in P, Ba and Mg and corresponded primarily to individuals caught off Mozambique, Somalia and Djibouti. These results are broadly consistent on one hand with patterns of water mass circulation in the Red Sea and western Indian Ocean and on the other hand with the observed spawning seasons. Though further research using, for example, archival tagging is needed to clarify the mechanisms behind these patterns, these results reveal the potential of otolith chemistry to provide insights into the spatio-temporal dynamics of narrow-barred Spanish mackerel.

Keywords: Marine functional connectivity / population structure / LA-ICP-MS / marine resource management / artisanal fisheries

1 Introduction

Though narrow-barred Spanish mackerel (*Scomberomorus commerson*) (Lacepède, 1800) is widely distributed in the tropical waters of the Indo-Pacific and the Red Sea (Collette and Russo, 1984), it is a particularly important species for artisanal fisheries in Djibouti, the Red Sea and the western Indian Ocean. The Indian Ocean Tuna Commission (IOTC) has found in recent stock status analyses that narrow-barred Spanish mackerel is overfished and/or experiencing overfishing at the scale of the entire Indian Ocean (Fu, 2020; IOTC, 2017). Localized overfishing and depletion of the species have been observed in the northwest Indian Ocean, Arabian Gulf and Persian Gulf (Grandcourt, 2013; Grandcourt et al., 2005; IOTC, 2018; Kaymaram and Vahabnezhad, 2013). To ensure the sustainability of this resource the scientific committee of the IOTC indicated the need to clarify the stock structure and to establish a strategic regional approach to the assessment and

*Corresponding author: mosougueh@gmail.com

management of narrow-barred Spanish mackerel (Grandcourt, 2013; IOTC, 2018). However, fragmentary and sometimes contradictory knowledge on the spatio-temporal stock structure of this species prevents the implementation of an effective management strategy. Knowledge of spatial structure is particularly essential for this species given that landings are shared among a large number of nations, but little is known about the connectivity (IOTC, 2018) and therefore the interdependence between local populations exploited by each nation. It is imperative to develop knowledge on the structure and the spatio-temporal dynamics of the narrow-barred Spanish mackerel to ensure the sustainability of this resource.

In the Indian and Pacific Oceans, narrow-barred Spanish mackerel displays significant genetic structure. In the south west Pacific, three main genetic stocks have been identified centered on northern Australia, Papau New Guinea and Fiji (Fauvelot and Borsa, 2011; Shaklee et al., 1990). In the western-central Pacific, the existence of a resident population has also been reported (Collette, 2001). In the Arabian Peninsula, microsatellite markers revealed the existence of two genetic stocks: a stock limited to the locality of Dhofar in the Arabian Sea south of Oman (presumed to be a resident population); and a second, widely-distributed stock that covers the four regions of the Arabian Peninsula (Gulf of Arabian, Gulf of Oman, Arabian Sea, Gulf of Aden) (Van Herwerden et al., 2006). However, an analysis of mitochondrial DNA found only a single genetic stock in the Persian Gulf, the Gulf of Oman and the Arabian Sea (Hoolihan et al., 2006). These conflicting results leave the structure of narrow-barred Spanish mackerel population in the northwest Indian Ocean and Red Sea in doubt, highlighting the need to develop a better understanding of its spatial dynamics. In this study, we address this information gap via analyses of the microchemistry of narrow-barred Spanish mackerel otoliths.

There are several methods that can be used to study fish dynamics at different spatial and/or temporal scales (Cadrin et al., 2013). Among them, analyses of otolith (calcified carbonate concretions situated in the inner ear of fish) chemical compositions is widely used to explore movements and habitat use of fish (Perrion et al., 2020; Radigan et al., 2018; Tanner et al., 2016). Otoliths are metabolically inert and considered to retain permanently any elements incorporated in their calcium carbonate matrix, thereby acting as an environmental monitor and archive (Campana, 1999; Thresher, 1999). The chemical composition of the material accreted over the lifetime of an individual serves as a natural marker to identify fish that have inhabited environments with distinct physiochemical characteristics (Kerr and Campana, 2014). Otolith chemical element accumulations have been linked to various environmental factors (e.g., chemical composition, salinity, and temperature) and fish physiology (e.g., age, growth, metabolism, and ontogeny). The underlying mechanisms behind their incorporation into otoliths are not yet completely understood, though certain elements are associated with specific abiotic or biotic mechanisms (Sturrock et al., 2012; Sturrock et al., 2015; Izzo et al., 2018). For example, the incorporation of Ba and Sr into otoliths is now well known as being influenced by ambient concentrations of these elements, temperature and salinity, and especially upwelling phenomena for Ba (Kingsford et al., 2009; Lin et al., 2013; Woodson et al., 2013; Wheeler et al., 2016; Walsh and Gillanders, 2018).

Otolith microchemistry has the power to discriminate among populations of fish with distinct spatial distributions over part or all of their life-history (Campana, 1999; Clarke et al., 2015; Elsdon et al., 2008; Panfili et al., 2018; Thresher, 1999). It has been widely used to assess migration strategies and the structure of fish populations (Bae and Kim, 2020; Sturrock et al., 2015; Tanner et al., 2016). In particular, studies have used otolith microchemistry to understand the stock structure of highly migratory tropical tuna populations in the Indian and Pacific Oceans (Artetxe-Arrate et al., 2019, 2021; Rooker et al., 2016), suggesting that much can potentially be gained from applying this approach to other pelagic species, such as narrow-barred Spanish mackerel.

Despite the value of otolith microchemistry for understanding the dynamics and structure of fish populations, no study has yet investigated the otolith microchemistry of narrow-barred Spanish mackerel. In this study, we examined the spatio-temporal structure of narrow-barred Spanish mackerel populations using otolith microchemistry from fish captured in the Red Sea and the western Indian Ocean. We analyze otolith chemical signatures at different points along the otolith, and therefore at different points in the life history of individual fish, including the point of capture and the larval phase. We then quantified the extent to which specific study sites and seasons of capture were associated with specific, identifiable chemical signatures. Finally, we placed the results in the context of understanding the spatial structure and temporal dynamics of narrow-barred Spanish mackerel, as well as the relevance of these for regional fisheries management.

2 Materials and methods

2.1 Study area

The sampling areas of this study were located in the Red Sea and the western Indian Ocean both north and south of the Equator (Fig. 1). With the exception of South Africa, the area was characterized by a tropical climate with reversed seasonal cycles with a wet summer and dry winter. In the Red Sea and the northwestern Indian Ocean, the summer season occurs between May and October, whereas the winter season takes place from November to April. In the Red Sea and the Gulf of Aden the sea surface temperature displays similar annual evolution, reaching its maximum values during the months of August and September (31 °C) while the minimum temperatures are reached in February (~24 °C) (Nandkeolyar et al., 2013). In contrast, in the south-west of the Indian Ocean, the seasonal cycles break down as follows: winter sets in from May to October and the summer season occurs November to March. In the Western Equatorial Indian Ocean (e.g., Mozambique), sea surface temperatures range between 26.5 °C in winter to 28.5 °C in summer (Jaswal et al., 2012). Sea surface temperatures along the east coast of South Africa for both summer and winter decrease steadily from North to South and range between 16 and 22 °C in winter and 18–27 °C in summer (Smit et al., 2013). The sampling regions belong to three distinct provinces based on the Longhurst (2007) biogeographical classification of the Pelagic Ecosystem and their dynamics (Reygondeau et al., 2013). The Mozambique Channel and eastern South Africa belong to the East African

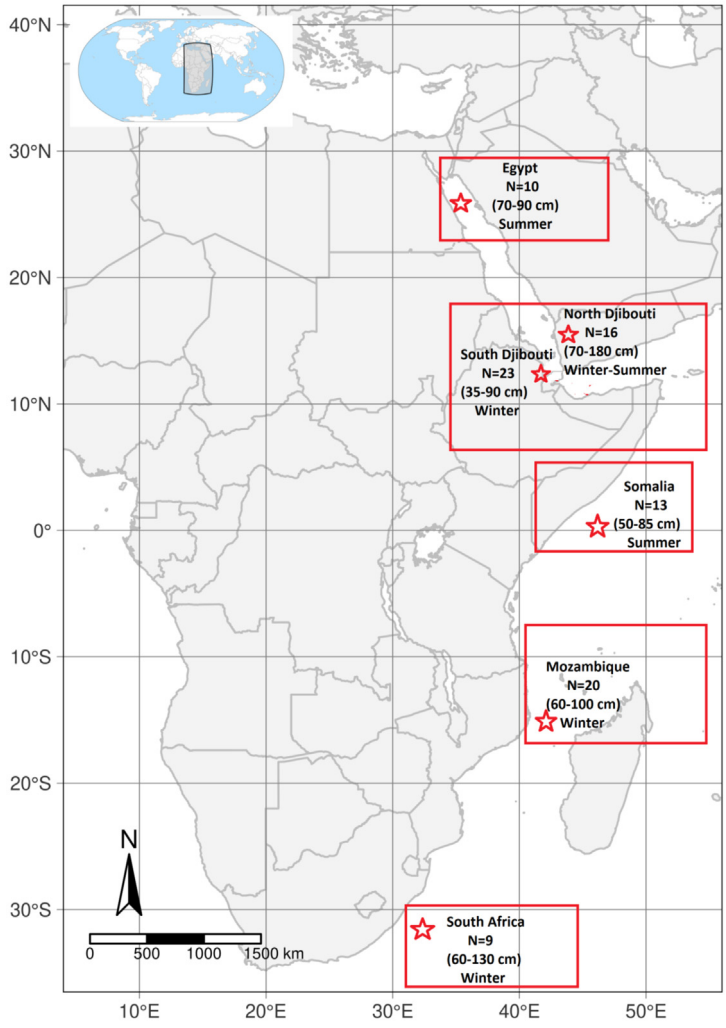

Fig. 1. Number of narrow-barred Spanish mackerel otoliths analyzed the sampling season and the size distribution of sampled individuals from each sampling location.

Coastal Province (EAFR), the Red Sea samples and Djiboutian samples are part of Red Sea and Arabian gulf province (REDS) and Somalian samples belong to the Trade wind Indian Northwest Arabian Sea upwelling province (ARAB). Importantly, Djibouti is located near the limits of the REDS and ARAB Longhurst provinces and water masses present in this area can vary as a function of monsoon driven changes in ocean circulation (Reygondeau et al., 2013).

2.2 Sample collection

Narrow-barred Spanish mackerel samples were collected from the Red Sea and western Indian Ocean on seven separate occasions (Tab. 1). In the Red Sea, all samples originating from southeast Egypt and north Djibouti were caught by local fishers using trolling and hand-lines from 2018 to 2020 (1st sampling occasion in north Djibouti in 2018, then in Egypt in 2019, and finally the 2nd sampling occasion in north Djibouti in 2020). In the western Indian Ocean, fish samples were caught by a mix of angling, trolling and hand-lines in four locations: Gulf of Aden in south Djibouti, Somalia, Mozambique and South Africa. Whereas individuals from south Djibouti and Somalia were caught by local fishers between 2018 and 2020, samples from Mozambique and South Africa were collected by the Oceanographic Research Institute (ORI) in 2011 as part of a previous study on the growth of narrow-barred Spanish mackerel (Lee and Mann, 2017). A total of 91 individuals were sampled and the breakdown of these individuals by sampling site, season and size range is presented in Table 1.

In the northern Indian Ocean, applying the estimated size at first sexual maturity (75 cm FL for combined sexes) (Devaraj, 1983), 60% of sampled narrow-barred Spanish mackerel were adults. For estimating age from size, we used the Von Bertalanffy curve obtained by Govender et al. (2006) for samples from Egypt, Djibouti and Somalia and that of Lee and Mann (2017) for samples from Mozambique and South Africa.

Table 1. Number, sampling period, size range and estimated ages of fish for all sampling locations. RS Red Sea; IO Indian Ocean.

Sampling location	Sampling event code	Number analyzed	Sampling period	Sampling season	Size range (cm)	Number of individuals of size class 70-90 cm	Estimated age (years)*
Egypt (North-RS)	Egy-S	10	May 2019	Summer	70–90	10	1–2
Djibouti-North (South-RS)	Dji-N-W	7	December 2018	Winter	160–180	0	12–14
Djibouti-North (South-RS)	Dji-N-S	9	June 2020	Summer	70–90	9	1–2
Djibouti-South (NW-IO)	Dji-S-W	23	March −Deccember2018	Winter	35–90	17	0.5–2
Somalia (NW-IO)	Som-S	13	August 2020	Summer	50–85	9	0.5–2
Mozambique (South-IO)	Moz-W	20	October 2011	Winter	60–100	13	0.5–3
South Africa (South-IO)	Sa-W	9	May 2011	Winter	60–130	2	0.5–10

* For fish sampled in Egypt, Djibouti and Somalia, the age estimates for males and females refer to the work carried out by Govender et al. (2006) in Oman and for fish caught in Mozambique and South Africa age estimates relate to the paper by Lee and Mann (2017) in the South West Indian Ocean (Mozambique).

2.3 Otolith preparation

The right sagittae otoliths were extracted from all 91 sampled individuals. All materials used for post extraction otolith handling, preparation and analysis were decontaminated in ultra-pure nitric acid baths (trace element quality) then rinsed with water and dried in a laminar flow hood class 100. Subsequently, the otoliths were cleaned from adherent tissues, rinsed with distilled water, then sonicated for 5 min in ultrapure water and dried under the same laminar flow hood. Then, the otoliths were included in Epoxy-Araldite resin and polymerized in an oven at 35 °C for 24 h. Finally, transverse cuts (1 mm thick on average) containing the core were made using a precision saw (Bluehler®, Isomet 1000). The otolith sections were then manually polished using 1200, 2400 and 4000 grit dry abrasive paper until the core was reached. In order to avoid contamination in the measurements of trace elements, the sanding papers were renewed between each sample. Finally, prepared sections were rinsed in deionized water, air dried overnight in a class-100 laminar flow cabinet and arranged in rows on microscope slides using double-sided tape.

2.4 Trace element analysis (LA-ICP-MS)

Otoliths were analyzed using laser ablation-inductively coupled plasma mass spectrometry (LA-ICPMS: FINNIGAN-Element2 XR coupled to an Excimer Analyte G2 193nm (Teledyne Cetac) laser) on the AETE-ISO OSU-OREME platform of the University of Montpellier, France. For each otolith, the concentrations were measured along a transect from the core to the edge along the ventral arm. A pre-ablation transect was conducted to minimize potential surface contamination (pulse frequency 4 Hz, speed 20 μm/s and a spot diameter of 85 μm) before performing the final ablation transect for measuring the chemical concentrations of chosen elements (pulse frequency 7 Hz, speed 15 μm/s and a spot diameter of 50 μm). For calibration, a glass reference material (NIST 612–National Institute of Standard and Technology, USA) was analyzed at the beginning, after every fifth sample and at the end of each session. Another reference material (MACS 3_United States Geological Survey) (Strnad et al., 2009) was analyzed at the beginning and at the end of each session to check measurements reproducibility. To remove residual sample gas that could interfere with the analysis, the laser chamber was purged for 30 seconds before analyzing each sample. Seventeen chemical elements were measured: ^{7}Li, ^{11}B, ^{224}Mg, ^{31}P, ^{52}Cr, ^{53}Cr, ^{55}Mn, ^{65}Cu, ^{66}Zn, ^{86}Sr, ^{89}Y, ^{138}Ba, ^{139}La, ^{140}Ce, ^{141}Pr, ^{208}Pb, ^{43}Ca.

Calcium was used as the internal otolith standard to correct for variation in ablation yield among samples and results were given as ratios to Ca. Finally data reduction and processing were performed using the elementR packages version 1.3.7 (Sirot et al., 2017) developed using the R programming language (R Core Team, 2018). This package corrected the machine drift using the reference materials, determined the levels of detection for each element and discarded outliers. Among the 17 chemical elements analyzed by LA-ICPMS, only four, Mg, P, Sr and Ba, were consistently above the detection limit and were retained for further statistical analyses. External precision (relative standard deviation) for the reference material (MACS-3) was as follows: Mg = 5%, P = 11%, Sr = 3% and Ba = 5%.

2.5 Statistical analyses

Before performing statistical analyses, a running average of length three (i.e., average across 3 spots) was applied to the otolith transect data from each individual to reduce noise. Using these smoothed data, preliminary analyses were performed to each transect to visualize the trajectories of each element as a function of distance from the otolith core (hereafter referred to simply as “otolith distance”) for each sampled individual. Based on estimates of the mean and standard deviation by sampling event of transect data as a function of otolith distance, differences between sampling events were observed and therefore subsequent analyses focused on placing individuals into clusters based on differences in chemical composition. Analyses focused primarily on each individual’s first (i.e., average of the first 3 spots of an individual’s otolith transect) and last (i.e., average of the last 3 spots of an individual’s transect) data points to examine and compare the chemical composition of the otolith core (larval phase) and period immediately preceding capture, respectively, among samples from different sampling event. Hereafter, these data will be referred to as the “core” and “capture” points, respectively.

As Shapiro-Wilk tests identified non-normality in the core and capture data, we used non-parametric statistics to analyze elemental concentration variations among individuals and sampling events. We used multivariate analysis of variation permutation (Permanova) with two crossed factors (sites and capture season) on the core and capture points to identify statistical differences among sampling events. Then, we performed principal component analyses (PCA) (Legendre and Anderson 1999) separately on core and on capture data of the 4 chemical elements to identify dominant axes of variability in the data. Though PCA analyses were initially performed using data from all sampled individuals (size range 35–180 cm corresponding roughly to 0.5–14 years), we subsequently limited the influence of size and age class differences by repeating the analyses only considering samples from individuals of size 70–90 cm (±2 cm; 1–2 years of age). This size class includes individuals commonly caught in fisheries and represented 66% of the samples used for this study. It excluded samples captured during winter in South Africa (Sa-W) and north Djibouti (Dji-N-W), thereby refocusing analyses primarily on samples captured in the northeast Indian Ocean and increasing homogeneity across sampling events in terms of number of individuals (Tab. 1). All PCA analyses and visualizations were performed using the FactoMineR and FactoExtra packages in R (Kassambara, 2017; Lê et al., 2008). Considering that samples from Mozambique and South Africa were collected in 2011 and in order to limit the spatio-temporal mismatch between samples, analyses were also carried out including only individuals caught in Egypt, Djibouti (North and South) and Somalia between 2018–2020. These analyses were done twice including all size class individuals and only including individuals in the 70–90 cm (±2 cm) size class. We then used agglomerative Ward's hierarchical clustering (Murtagh and Legendre, 2014) on the PCA results to identify samples who shared similar elementary signatures (otolith elemental signatures are also referred to as the otolith chemical fingerprints; e.g., Artetxe-Arrate et al., 2021) at the otolith capture or core points. Hierarchical clustering was based on Euclidean distances between the principal components coordinates of the centered and reduced data for individuals and carried out using the HCPC function of the FactoMineR package (Murtagh and Contreras, 2017). The identification of the optimal number of clusters was carried out in R using the Euclidean Criteria in the NbClust package (Charrad et al., 2014). Finally, the projections of individuals on the different clusters were visualized using the fviz_cluster function in the FactoExtra package (Kassambara and Mundt, 2017).

In order to assess the stability of group assignment over the life cycle, smoothed elemental data (i.e., 3-spot running averages) from along the otolith transects were projected onto the principal components from the PCA analysis of capture point data. This allowed us to visualize individual transects over the life cycle in this PCA space, as well as assess the stability of group assignments by calculating the barycenter of the previously determined groupings as a function of otolith distance relative to the capture point.

This analysis was limited to individuals in the 70–90 cm (±2 cm) size class to have a relatively homogeneous sample and the examined data was limited to a fixed maximum distance from the otolith edge to assure that data used for the individual with the smallest otolith was at least 500 μm from the otolith core. This distance was used as the cutoff as, based on visual inspection of individual chemical compositions as a function of distance, this distance corresponded approximately to the part of the otolith concerned by the early life history phases (e.g., peak in presence of certain elements not seen at larger distances).

3 Results

3.1 Profiles of chemical concentration variations

The pattern of variations in elemental chemical concentrations along individual otolith transects varied by element, sampling site and season. For all samples, mean P concentration reached a peak around the otolith core (Fig. 2). This peak was more pronounced for samples caught in Djibouti north (Dji-N-W), Djibouti south (Dji-S-W), Mozambique (Moz-W) and South Africa (Sa-W) with an overall average value of 3.5×10□ ppm. For samples caught in Egypt (Egy-S), Djibouti north (Dji-N-S) and Somalia (Som-S), the peak value did not exceed an average of 1.5×10□ ppm. In addition, in the later set of samples (Egy-S, Dji-N-S, Som-S) corresponding to juvenile individuals (<75 cm) caught in summer, P levels were relatively stable along the transect. In contrast, for the former set of samples (Dji-N-W, Dji-S-W, Moz-W, Sa-W), mean P displayed stronger variation among and within individuals. Further, *P* values were higher than the mean observed for all other fish during the juvenile part of the otolith (<1500 μm from core based on the typical 70–90 cm size of individuals caught with this size otolith). Only fish sampled from Djibouti north (Dji-N-W) presented the same mean for the adult part of their otolith transects as did the juveniles caught in summer in the same area. These observations suggested a link between chemical composition and sites that seems to be persistent throughout the life cycle of sampled individuals.

The other elemental signatures examined showed similar overall tendencies of having more variability in individuals captured in winter than in summer, though each season had its own particularities (Online Supplementary Figs S1, S2 and S3). Mg concentration showed a similar pattern to P with a peak in the otolith core decreasing and then stabilizing at around 1000 μm (Fig. 3). In contrast, Sr showed a very different pattern with a dip at around 500 μm followed by an increasing trend afterward (Fig. 4). The exceptions to these trends are Dji-N-W samples, for which the stabilization of Mg values appeared to happen later at around 2500 μm. The dip in Sr occurred at around 1500 μm; the Sr dip was wider and more pronounced for South Africa samples. Results for Ba indicated generally stability along the otolith transect with an overall mean value $<1.5 \times 10^{-5}$ ppm (Fig. 5). Exceptions to this were the samples from Dji-N-W, which peaked between 500 μm and 1000 μm at $\sim 3.5 \times 10^{-5}$ ppm before declining and stabilizing at around 1.0×10^{-5} ppm, and samples from Moz-W with a lower peak ($\sim 1.0 \times 10^{-5}$ ppm) at around 250 μm followed by a decreasing trend afterward.

3.2 Capture point analyses

Using capture point concentrations, the multi-element Permanova test (Mg, P, Sr and Ba) with factors site and season showed significant effects for both site ($p < 0.001$; $F = 16.24$;

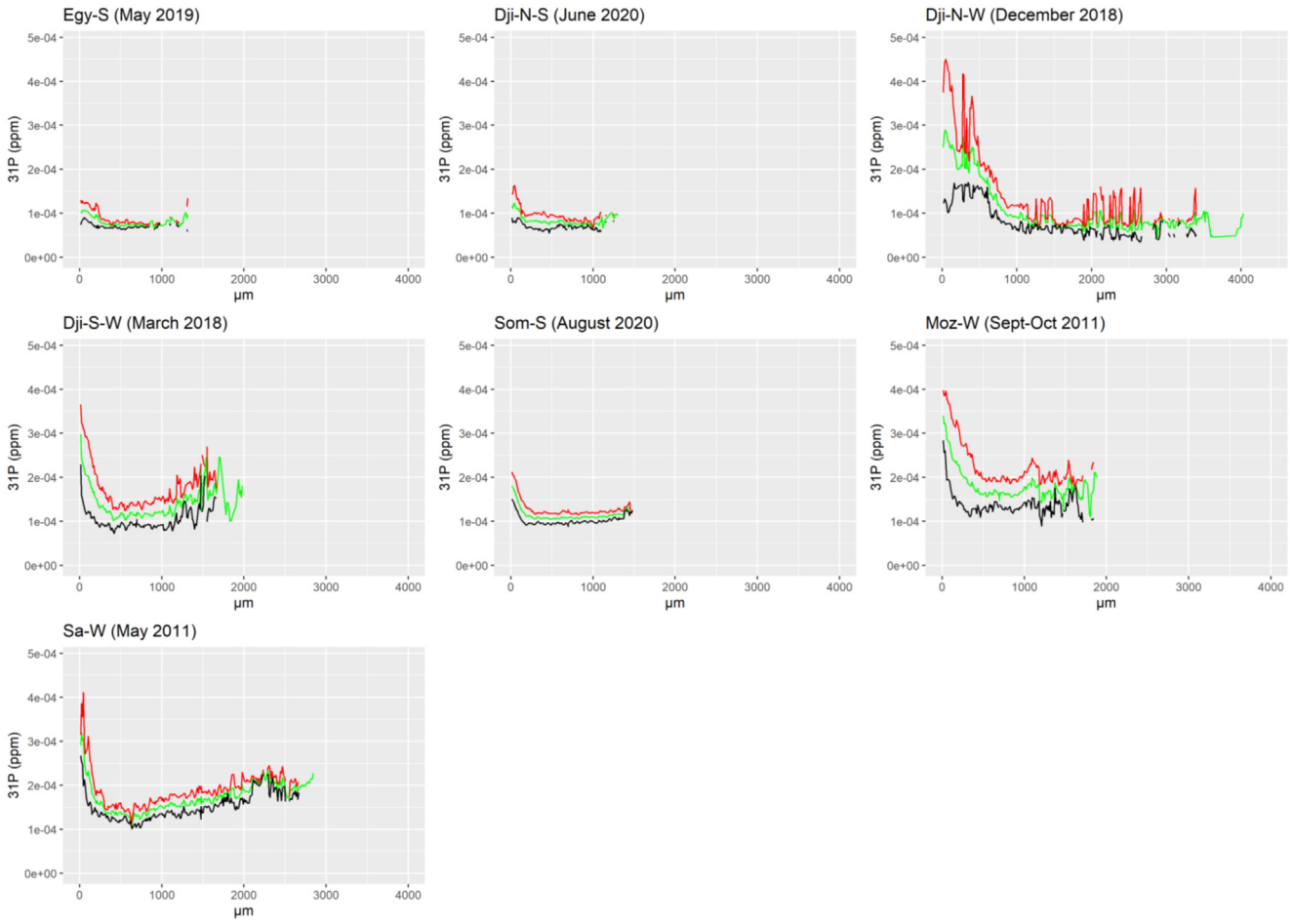

Fig. 2. ^{31}P trace element concentrations measured along transects ablated from the otolith core to the terminal edge for all samples. The mean variation across individuals is represented by green curve, +1 standard deviation by the red curve and −1 standard deviation by the black curve. Please refer to Table 1 for the acronyms used to identify sampling events.

df = 5) and season ($p = 0.027$; $F = 2.75$; df = 1). The results indicated thus significant spatio-temporal differences in otolith chemical compositions among sampling events.

The PCA analysis for capture points of all sampled individuals allowed us to distinguish between sampling events in ways that were consistent with specific effects of geographical proximity and sampling season. The first two principal components explained 68.8% of the total variance (Fig. 6). Elements P, Ba and Mg contributed positively to the first component. The second principal component was strongly positively influenced by Sr and to a lesser degree negatively influenced by Mg. In general, individuals caught in winter from Djibouti and Mozambique had a positive first principal component with considerable variability among individuals and sampling events, whereas samples caught during summer in Egypt, Djibouti and Somalia had a negative first principal component and somewhat less variability among individuals and sampling events (blue versus red points in Fig. 6). Thus the first axes separated winter and summer samples.

For all samples, agglomerative Ward's hierarchical clustering on capture points identified two clusters (Figs. 7a, 7b). Cluster 1 was mainly composed of a mix of fish caught during summer in Egypt (Egy-S; 100%), Djibouti north (Dji-N-S; 100%) and Somalia (Som-S; 100%) and fish caught during the winter in Djibouti north (Dji-N-W; 100%), Djibouti south (Dji-S-W; 95%) and surprisingly South Africa (Sa-W; 100%). Cluster 2 predominately contained samples caught during winter in Mozambique (Moz-w; 85%) and Djibouti south (Dji-S-W; 5%). Both clusters were characterized by multi-elementary signatures that were significantly distinct for all elements (all p-values < 0.001). Limiting these analyses to samples from Egypt, Djibouti and Somalia collected in 2018–2020 but still considering all size class, agglomerative Ward's hierarchal clustering on capture points produced five clusters that were difficult to interpret (Online Supplementary Figure S2A, a).

For individuals in the 70–90 cm size class, agglomerative Ward's hierarchical clustering on capture points identified three clusters (Figs. 7c, 7d). Cluster 1 was made up mainly of fish sampled in the summer season in Egypt (Egy-S; 90%), Djibouti north (Dji-N-S; 100%) and Somalia (Som-S; 100%). Cluster 2 exclusively contained samples caught in Djibouti south during winter (Dji-S-W; 100%) and cluster 3 covered all the individuals sampled in Mozambique (Sa-W; 100%). Again, all clusters were characterized by multi-elementary signatures that were significantly distinct for each individual element (all p-values < 0.001). As the samples from Mozambique were captured in 2011, 7–9 years before the samples from the

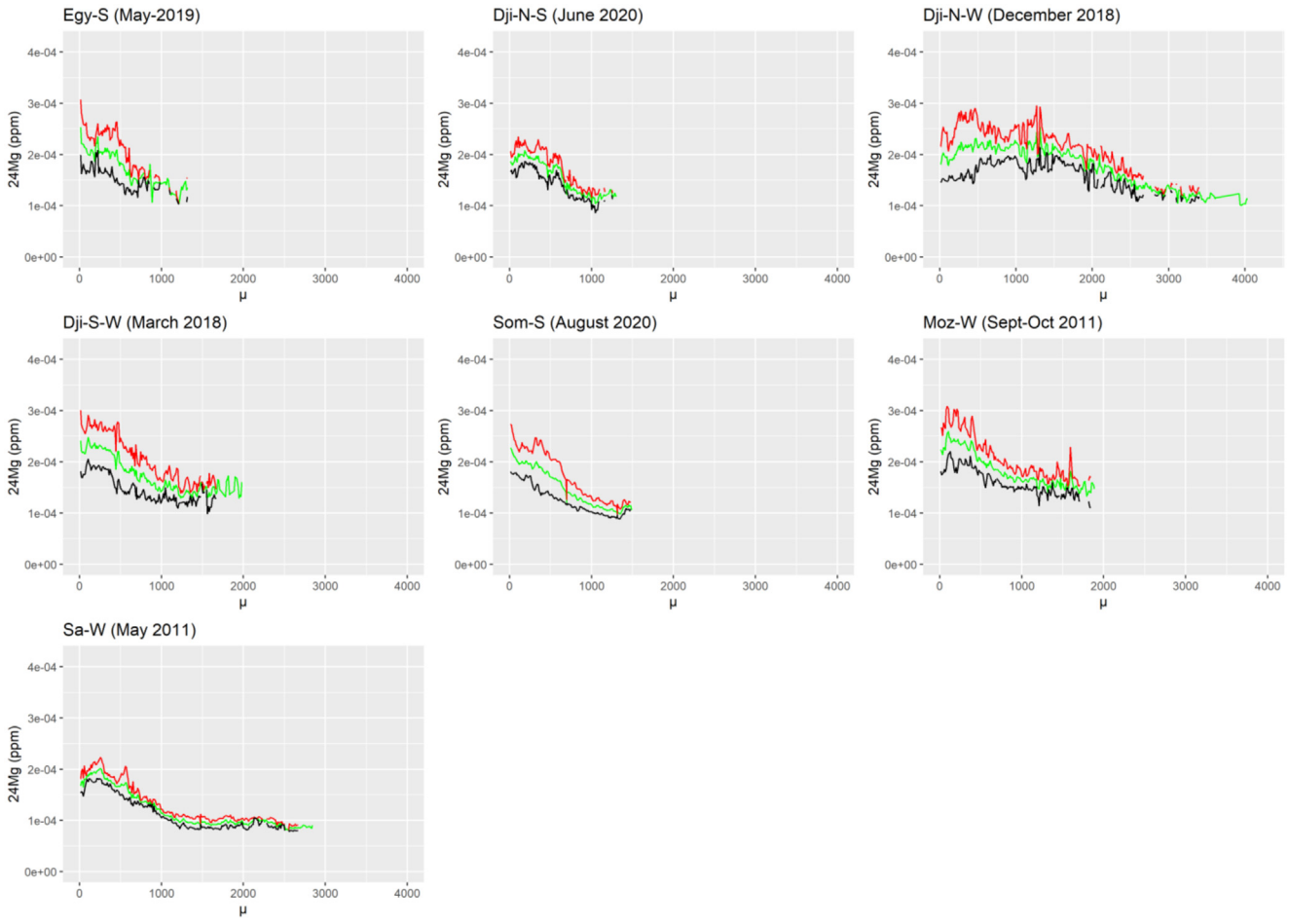

Fig. 3. ^{24}Mg trace element concentrations measured along transects ablated from the otolith core to the terminal edge for all samples. The mean variation is in green, +1 standard deviation in red and −1 standard deviation in black. Please refer to Table 1 for the acronyms used to identify sampling events.

northern hemisphere, we redid the same analysis limiting samples to those from the northern hemisphere collected in 2018–2020. The compositions of the first two clusters were the same as those presented in Figure 7c (Online Supplementary Figs S2 c, d)

For individuals in the 70–90 cm size class, projection of the elemental data (otolith transect distance at least >500 μm) onto the principal components from the PCA analysis of the capture points data allowed us to track both individual elemental histories and the barycenters of each of the three clusters (Fig. 8). Moving in the direction of the otolith core, the barycenters of cluster 1 (Egy-S, Dji-N-S, Som-S) and cluster 3 (Moz-W) and to a lesser degree cluster 2 (Dji-S-W) became progressively more negative on the second PCA. This was due to lower values for Sr and, to a lesser degree, Ba. Barycenters of cluster 1 remained slightly separate from those of clusters 2 and 3. These latter two clusters started to superimpose as otolith transect distances approached 500 μm from the core.

3.3 Otolith cores analysis

Results for the multi-element Permanova test (Mg, P, Sr and Ba) with factors site and season using data from otolith cores indicated significant effects for both site ($p < 0.001$; $F = 5.20$; df = 5) and season ($p < 0.001$; $F = 8.50$; df = 1). Moreover, multiple comparisons of the mean elemental signatures of otolith cores points indicated significant differences among samples according to the sample season and location (Fig. 9).

The PCA analysis for otolith core points generally allowed us to separate sampling events based on geographical proximity and season of capture, though samples caught in Djibouti South (Dji-S-W) had widely varying otolith core chemistries leading it to superpose with a number of other sampling events (Fig. 10). The first two principal components explained 65.8% of the total variance for all sampling event and 67.8% for the PCA analysis limited to samples from Egypt, Djibouti and Somalia. Elements P, Ba and Mg contributed positively to the 1st PCA component, while Sr influenced it negatively. The second principal component was positively influenced by Sr, Ba and P, while Mg influenced it negatively. The barycenters of otolith core signatures from sampling events in summer tended to have a negative first and second principal component, whereas those captured in winter had a positive first and second principal component with the exception of samples caught in Djibouti south (Dji-S-W) (Fig. 10).

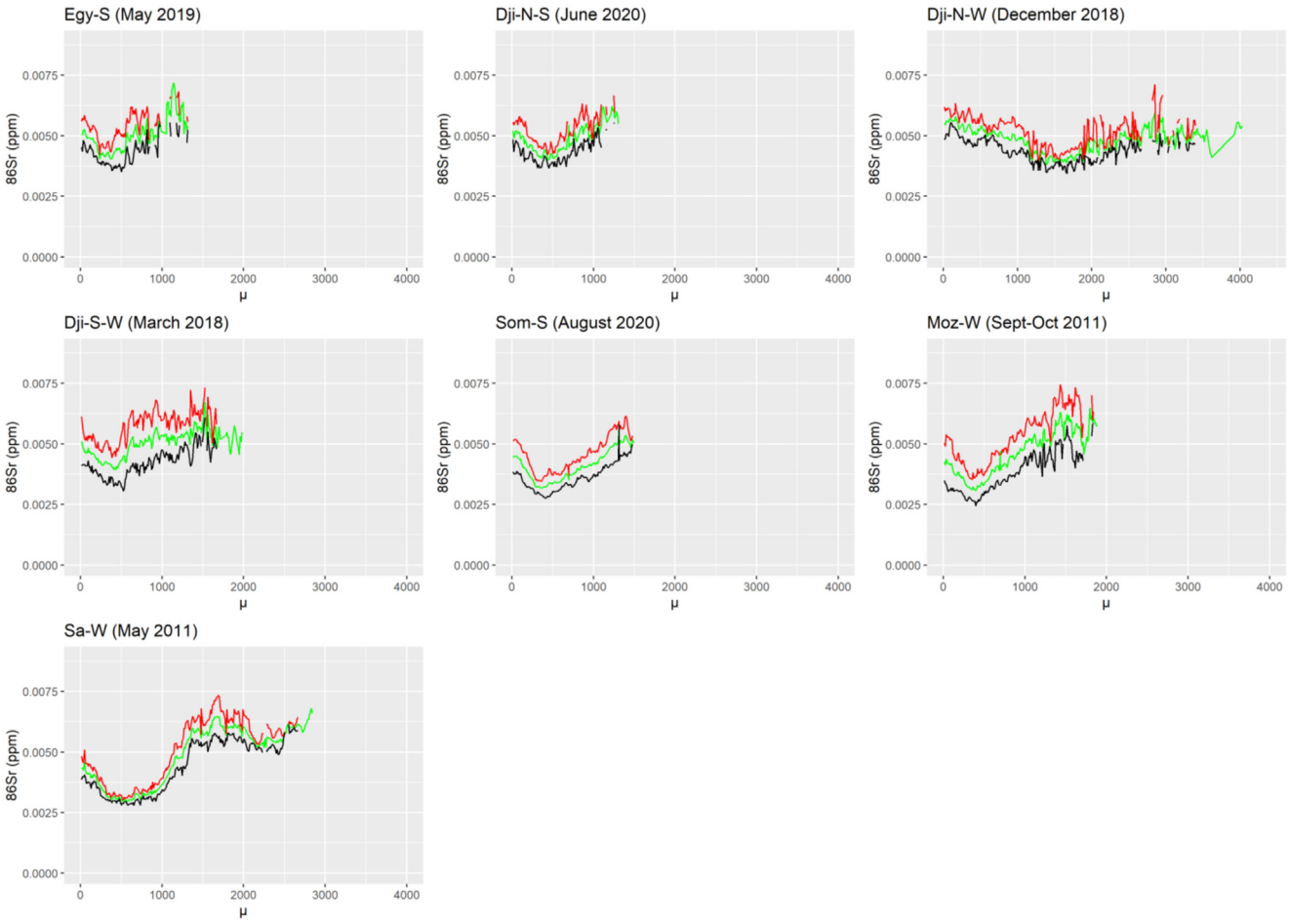

Fig. 4. ^{86}Sr trace element concentrations measured along transects ablated from the otolith core to the terminal for all samples. The mean variation is represented in green, +1 standard deviation in red and −1 standard deviation in black. Please refer to Table 1 for the acronyms used to identify sampling events.

When all sampling events were taking into account, hierarchical clustering analyses produced two clusters characterized by distinct signatures for each of the trace elements (p-values < 0.001) (Fig. 11a). Cluster 1, characterized by relatively high concentrations of Ba and Mg and low concentrations of Sr is more less prevalent in these following sampling event: 35% (Dji-S-W), 54% (Som-S) and 45% (Moz-W). Cluster 2, containing relatively high concentrations of Sr and low concentrations of Ba and Mg, was prevalent in all sampling events, but dominant among samples caught in Djibouti north (Dji-N-S; 100% Dji-N-W; 86%), Egypt (Egy-S; 70%) and South Africa (Sa-W; 89%).

Analyses of core point elemental signatures limited to samples from Egypt, Djibouti and Somalia (without samples from Mozambique and South Africa) produces two clusters (Fig. 11c). Cluster 1 was characterized by relatively low concentrations of Ba, Mg and Sr and made up primarily of fish caught during summer in Egypt (Egy-S; 100%), Djibouti north (Dji-N-S; 100%) and Somalia (Som-S; 100%) and a considerable part of fish caught during winter in Djibouti north (Dji-N-W; 29%) and Djibouti south (Dji-S-W; 78%). Cluster 2, characterized by relatively high concentrations of Ba, Mg and Sr was composed exclusively by fish caught during winter in Djibouti north (Dji-N-W; 71%) and Djibouti South (Dji-S-W, 22%).

4 Discussion

Improving our understanding of the spatio-temporal dynamics of exploited species is essential for defining appropriate management strategies and optimizing the use of fishery resources. The chemistry composition of otoliths is strongly influenced by the environment and can be used to discriminate among populations of fish in geographic areas with environmental characteristics that display spatial or seasonal variations (Campana, 1999; Elsdon et al., 2008; Kitchens et al., 2018; Rogers et al., 2019). For the first time, this study examined otolith microchemistry for samples from narrow-barred Spanish mackerel in the Red Sea and the western Indian Ocean. Results highlighted the potential of this technique to provide valuable information about the species' spatio-temporal dynamics.

For groups of individuals in the 70–90 cm class (starting to become mature), the analysis on capture point data successfully clustered most individuals sharing season of capture and/

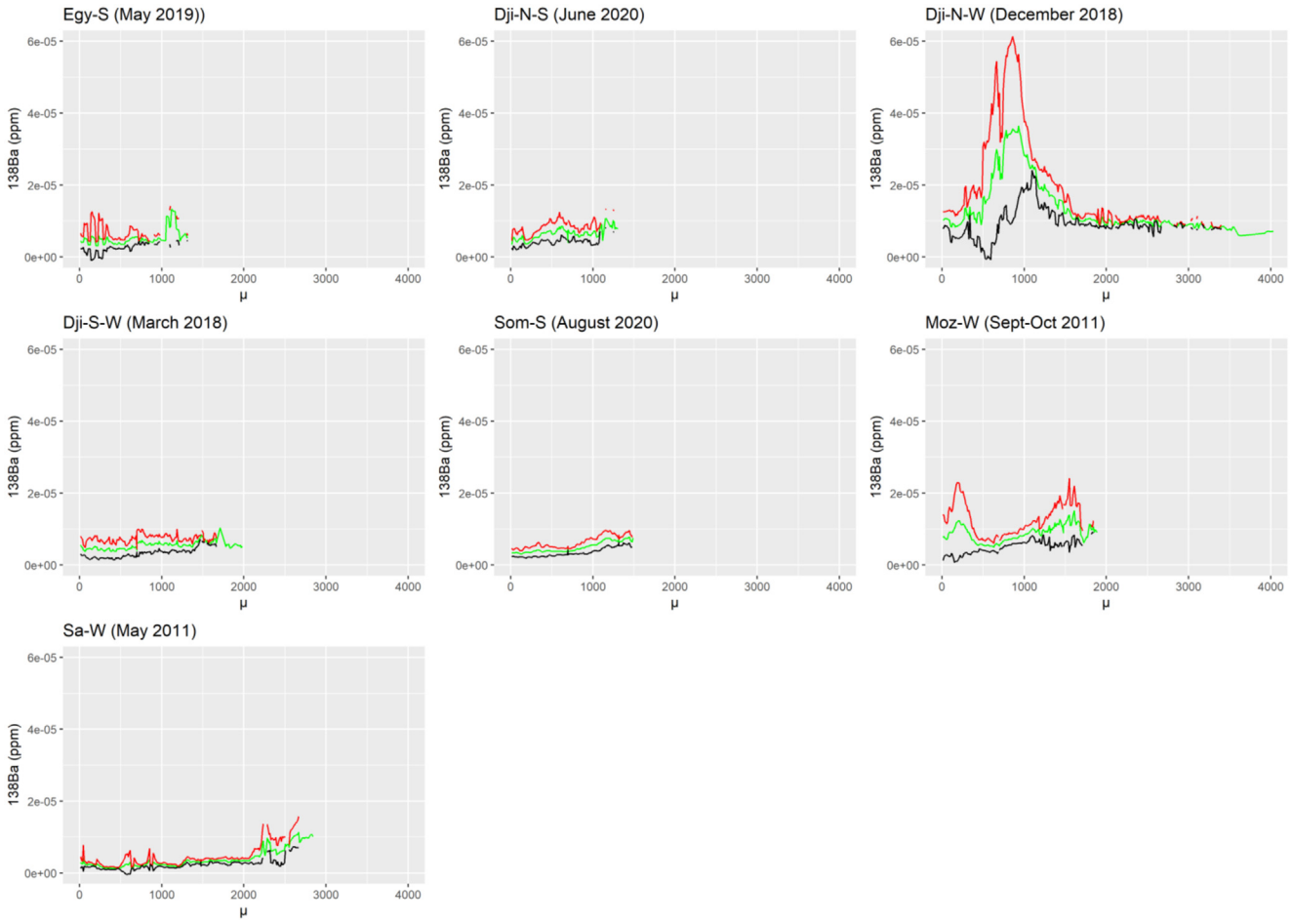

Fig. 5. ^{138}Ba trace element concentrations measured along transects ablated from the otolith core to the terminal edge for all samples. The mean variation in green, +1 standard deviation in red and −1 standard deviation in black. Please refer to Table 1 for the acronyms used to identify sampling events.

or spatial proximity, independent of capture year. Clustering results became more complex to interpret when all sampled individuals were taken into account. The size range of fish analyzed was large, ranging from 35 cm to 180 cm. With such a large range in size (and age), it is possible that otolith capture points chemistries did not present the same temporal and spatial levels of aggregation. Indeed, the data points obtained by averaging across three spots with constant diameter represented larger time scales for individuals older. Furthermore, ontogenetic effects and age-related differences in exposure history may result in very different chemical fingerprints for fish of different size-classes from the same population (Papadopoulou et al., 1980). Moreover, recent studies have indicated that although otolith element patterns reflect environmental concentrations, they can be influenced by physiological processes, typically exhibiting decreasing incorporation with increasing growth and age (Hüssy et al., 2020). As such, results including all sampled individuals must be interpreted with caution.

The analysis for capture points limited to fish in the 70–90 cm size class showed that samples captured in Somalia, North Djibouti and Egypt during summer were clustered together and characterized by low concentrations in Ba, P and Mg, whereas samples from South Djibouti during winter had relatively high concentrations of these elements. The Red Sea presents a seasonal reversal of monsoon-associated winds that create seasonally-varying circulation patterns in the southern Red Sea responsible for seawater exchange between the Red Sea and the Gulf of Aden through the Bab Al-Mandab Strait (Zubier, 2010). During the winter monsoon (November–April), wind driven water exchanges between the Gulf of Aden and the Red Sea correspond to a bilayer system with a strong surface current from the Gulf of Aden into the Red Sea and a subsurface counter current with high salinity moving in the opposite direction (Fersi, 2016). During the summer monsoon (May–October), the surface circulation reverses as winds push a layer of warm, salty surface water from the Red Sea into the Gulf of Aden, while dense, less salty, but colder, subsurface water from the Gulf of Aden enters the Red Sea (Fersi, 2016; Sofianos and Johns, 2007; Yao et al., 2014). During summer, the waters from the central region of the Gulf of Aden flowing into the Red Sea are known to be characterized by a strong downwelling caused by a mesoscale anticyclonic eddy, which in turn leads Chl-*a* and nutrients concentrations to drop

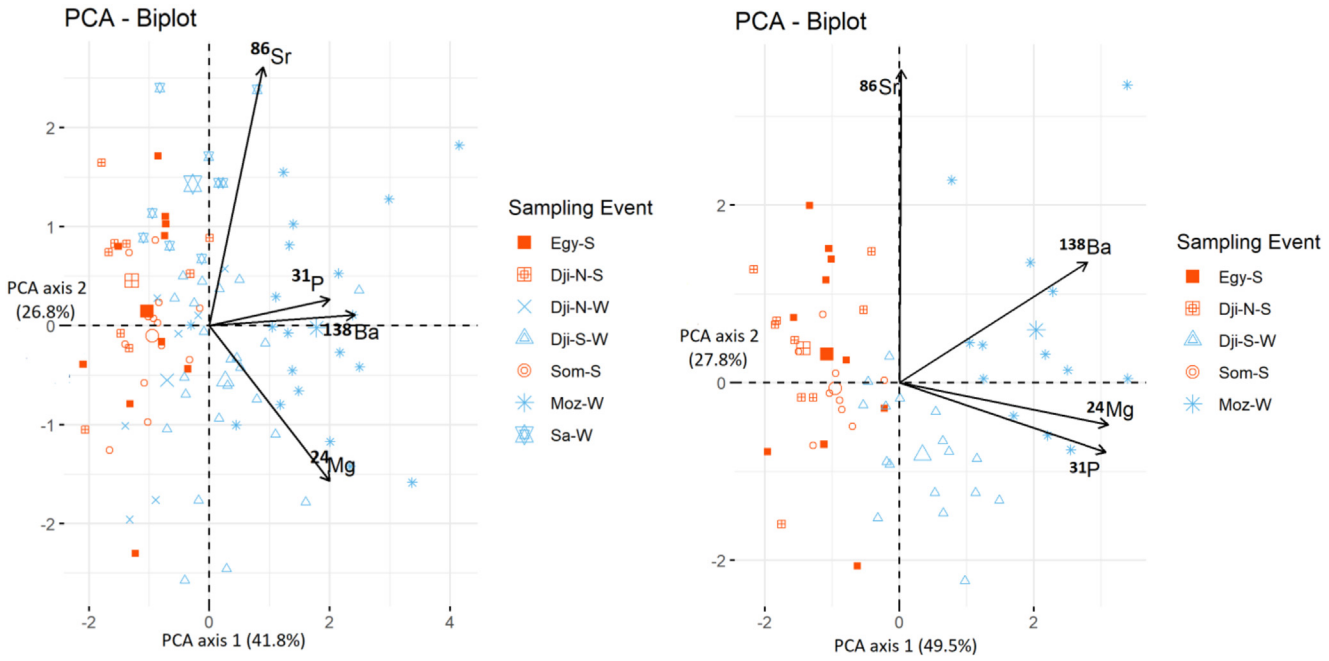

Fig. 6. PCA results made with otolith capture points signatures . First two PCA axes of trace element concentration signatures (^{24}P, ^{31}Ba, ^{86}Sr and ^{138}Mg) for all narrow-barred Spanish mackerel samples (left) and only for samples 70-90 cm (right). Sampling events are: Egypt in summer (Egy-S), North Djibouti during summer (Dji-N-S), North Djibouti in winter (Dji-N-W), South Djibouti in winter (Dji-S-W), Somalia in summer (Som-S), Mozambique in winter (Moz-W) and South Africa in winter (Sa-W). Fish sampled in winter are in blue and fish caught in summer in red. The black arrows represent the contribution of each trace element to the first two PCA axes.

(Gittings et al., 2017). These known circulation patterns are consistent with the observed low concentrations in Ba, P and Mg in samples caught during summer in Djibouti and Egypt (barium levels are known to be poor in the open ocean but rich in upwelling areas; Hampton et al., 2018; Lin et al., 2013). In contrast, similarly low elemental concentrations found in samples from Somalia in August 2020 are more difficult to explain, as the Somali coast in summer is one of the most important upwelling centers in the entire Indian Ocean (Schott et al., 2009). Possible explanations for this discrepancy include the last three spots on the otolith transect actually representing somewhat earlier periods of the year before the onset of upwelling off Somalia in July, localized variability in upwelling intensity and/or fish migratory movements for reproduction (or other reasons) shortly before capture (Claereboudt et al., 2005). In Djibouti, it is noteworthy that samples captured during winter and summer seasons were characterized by different chemical signatures. This is likely linked to variations in water masses between summer and winter due to the monsoons. Nevertheless, regional artisanal fishermen consider that the fish encountered in Djibouti during summer consist primarily of individuals migrating into the zone from elsewhere. Therefore, it may be that migration plays a role in these differing chemical signatures and contrasting patterns, with permanent resident fish, which are considered by fisherman to be less abundant, mostly sampled in winter and migratory fish leaving the Somalia Coast and moving into Djibouti waters during summer. Additional future research in the areas of Djibouti and Somalia based on multiple sampling events at different times throughout a single year, and in combination with regional oceanographic data and archival tagging to track fish movements, should be carried out to help determine how these two processes, seasonal changes in water masses and potential migration, shape variability in otolith trace element concentrations. Samples caught in Mozambique in October 2011 clearly separated from those of other sampling events, presenting higher concentrations of Ba, P and Mg. These results are consistent with the observed upwelling that takes place during this time period in Mozambique and that is known to be characterized by high biological productivity and nutrients (P and Mg), for which Ba is a marker. Indeed, the Mozambique Channel is characterised by the presence of anticyclonic eddies that generate an upward movement of nutrient-rich waters around their edge, and advection of nutrient-rich coastal waters when they run along the coast (Quartly and Srokosz, 2004; Tew Kai and Marsac, 2010). Upwelling hotspots take place along northern and southern Mozambique (Vinayachandran et al., 2021a) and display seasonal variation between persistent downwelling (warm water) between April−July and intermittent upwelling events (cool water) between August−March (Malauene, 2010).

The otolith capture points for samples caught in South Africa had varying chemistries and mostly clustered with samples caught in Djibouti South during winter and, to a lesser degree, with samples caught in Djibouti North during winter. These results are difficult to interpret given the large spatial and temporal separation between these sampling events. We hypothesize that this may be related to individuals from different hemispheres having similar life-history strategies, but additional work considering individuals captured at similar time periods would be needed to test this hypothesis.

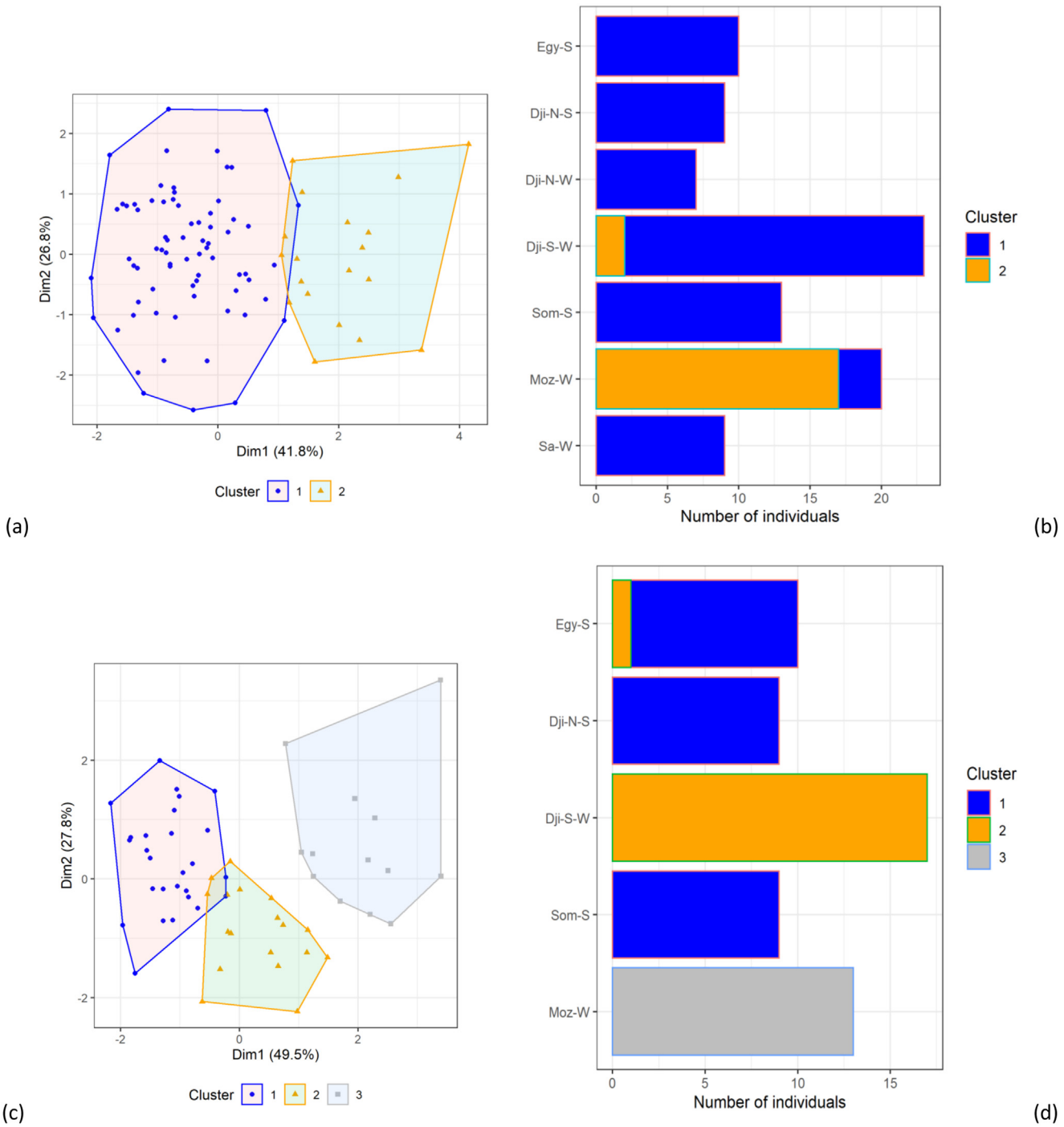

Fig. 7. Clusters obtained using agglomerative Ward's hierarchal clustering applied to the last three points of the otolith transects (capture point) including all samples (a) and including only samples of sizes 70-90 cm (c). Barplots on the right (b, d) indicate the number of individuals from each sampling event that were assigned to the different clusters with (b) corresponding to the clusters in (a), and (d) corresponding to the clusters in (c). The x-axis on the barplot represents the number of individuals for each sampling event colored by their assigned cluster.

The chemical compositions in PCA space when moving from the point of capture to the otolith core (Fig. 8) indicated that the barycenter of samples from Mozambique overlapped those of the cluster made up by samples from Djibouti caught in winter. As this species is known to be highly migratory (Grandcourt et al., 2005), it may be possible that individuals from both sites pass through similar ecological and environmental conditions in their life history, with or without physical superposition in space and time. Nevertheless, the large temporal separation between the sampling events in these two localities complicates interpretation of these results.

Given that otolith elemental signatures can be useful to backtrace the spawning origin of individuals (Farias et al., 2022; Thorisson et al., 2011), we used the otolith core

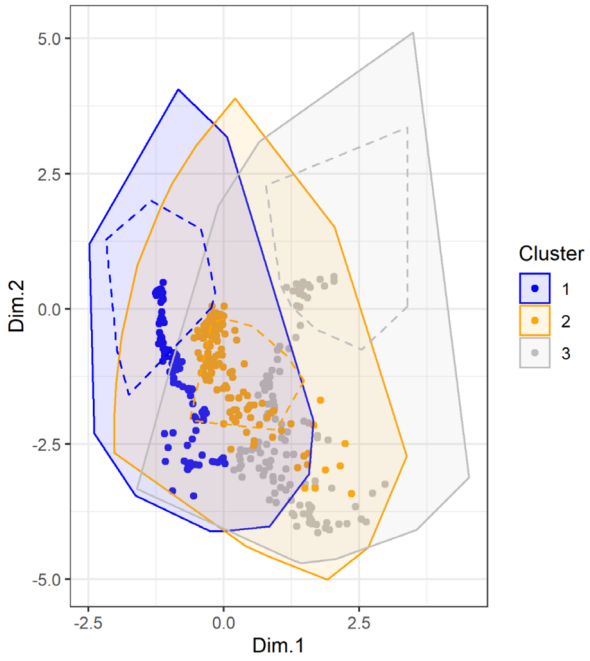

Fig. 8. The smoothed elemental data (otolith transect distance >500 µm from the otolith core) for sampled individuals in size class 70–90 cm projected onto the principal components from the PCA analysis of the capture points data (Fig. 7c). Points represent the barycenters by cluster of all individual fish in the sample at a given distance from the capture point, whereas solid enclosing polygons and shading represent the convex hull of all data for the corresponding cluster (i.e., for all distances from the capture point and all sampled individuals). Data are colored by cluster as in Fig. 7c . The polygons indicated by the dashed curves represent the capture point convex hulls for each cluster.

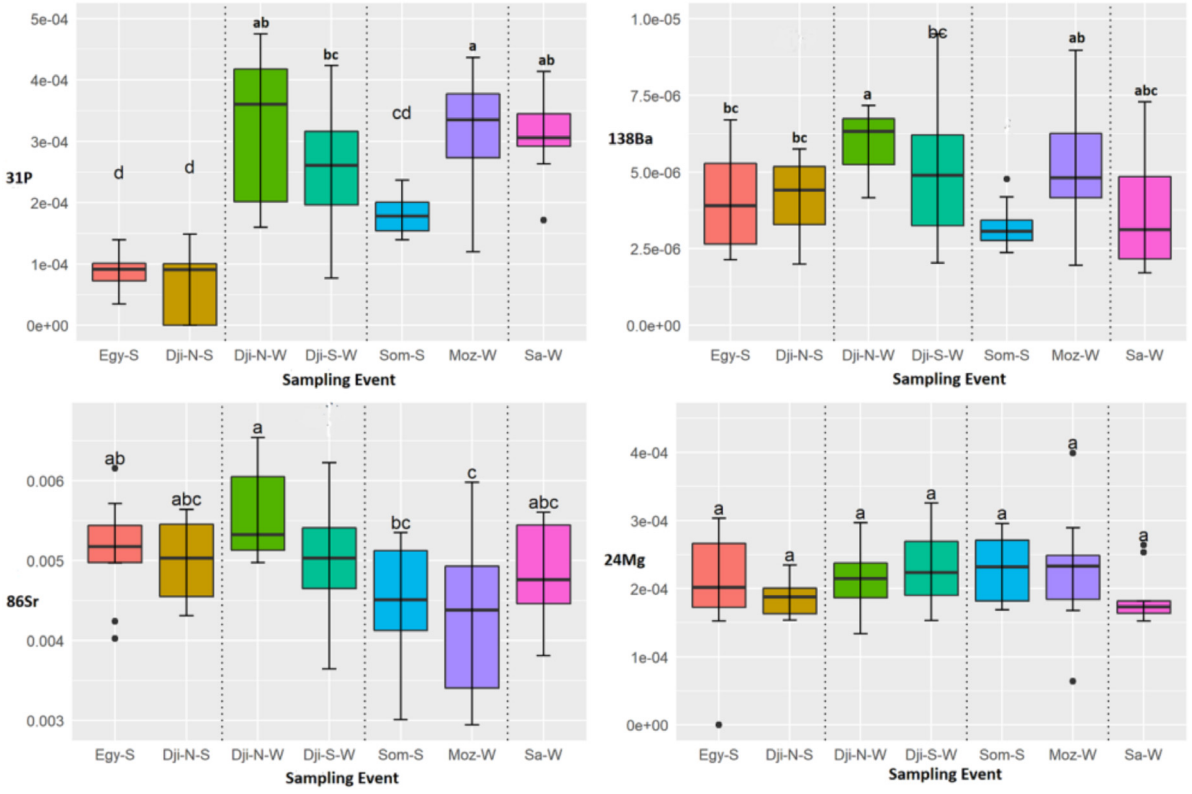

Fig. 9. Boxplots for the mean near-core chemical elemental signatures (^{31}P, ^{138}Ba, ^{86}Sr and ^{24}Mg) for all samples. Pairwise comparisons among sampling events for each trace element are represented by letters. Among sampling events, when the events share a letter, there is no significant difference between them. Horizontal lines indicate median values. Within the boxes, the upper lines indicate the quartile 3 and the lower lines indicate the quartile 1.

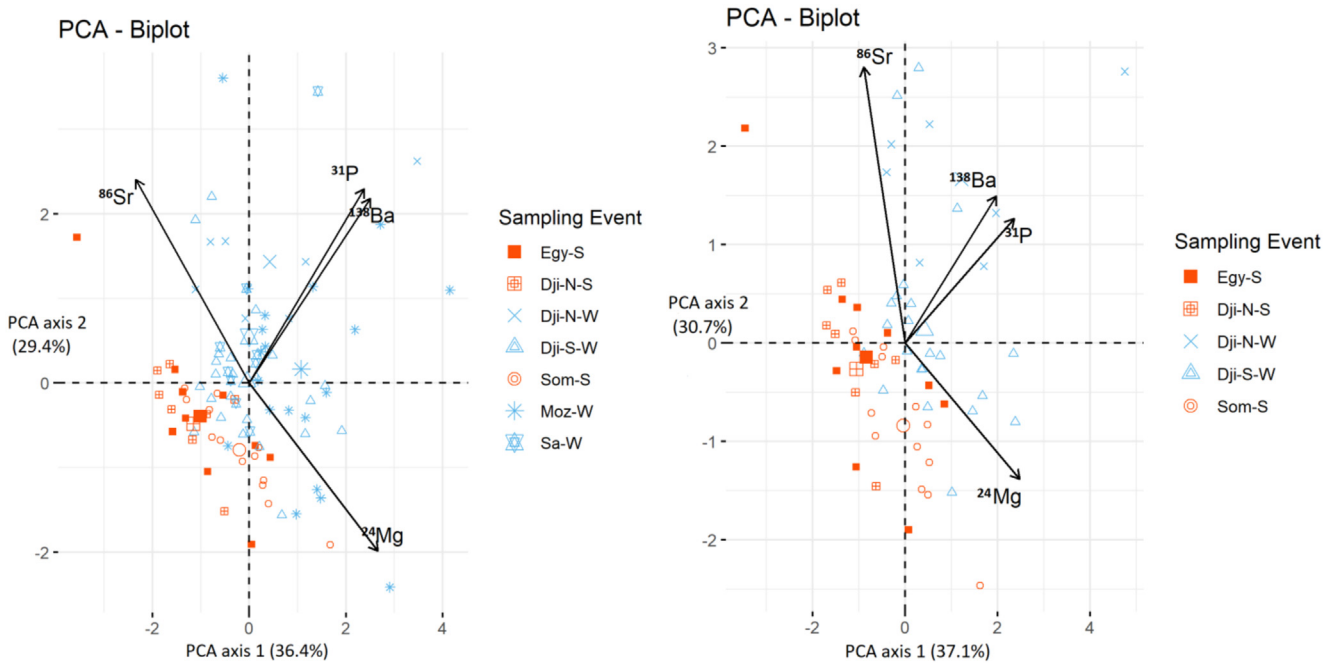

Fig. 10. PCA results made with otolith near-core signatures . First two PCA axes of trace element concentration signatures (^{24}Mg, ^{31}P, ^{86}Sr and ^{138}Ba) for all narrow-barred Spanish mackerel samples (left) and only for samples 70-90 cm (right). Sampling events are: Egypt in summer (Egy-S), North Djibouti during summer (Dji-N-S), North Djibouti in winter (Dji-N-W), South Djibouti in winter (Dji-S-W), Somalia in summer (Som-S), Mozambique in winter (Moz-W) and South Africa in winter (Sa-W). Fish sampled in winter are in blue and fish caught in summer in red. The black arrows represent the contribution of each trace element to the first two PCA axes.

chemistry to compare early life chemical signatures of sampled individuals. The results indicate two potential spawning origins, here referred to as SpO1 and SpO2:

– SpO1: Represented in all sampling events and mainly including fish caught during summer in Egypt (Egy-S), Djibouti north (Dji-N-S), Somalia (Som-S) and fish sampled in winter from Djibouti north (Dji-N-W), Djibouti south (Dji-S-W) and South Africa (Sa-W) (Tab. 2). Samples from this spawning origin were characterized by high concentrations of Sr and low concentrations of Ba and Mg. By taking into account the fact that Sr and Ba incorporation into otoliths are correlated with ambient water concentrations (Izzo et al., 2018) and that ^{13}Ba content of the ocean is more abundant in upwelling than in non-upwelling zones (Lin et al., 2013b; Wang et al., 2009), our hypothesis is that SpO1 corresponds to narrow-barred Spanish mackerel spawning grounds characterized by weak or non-existent upwelling. One such potential spawning ground is the central region of the Gulf of Aden where downwelling is observed during summer (Gittings et al., 2017). In Oman and the Arabic sea, this hypothesis is consistent with studies suggesting that at least some part of the narrow-barred Spanish mackerel population undertakes a spawning migration out of local coastal waters during summer (March–July; Claereboudt et al., 2005). Narrow-barred Spanish mackerel from eastern Australia are known to migrate and congregate in large numbers around several reefs just prior to spawning in the spring (Welsh et al., 2002). Similar large-scale migrations have also been reported for *Scomberomorus cavalla* in the Atlantic (Sutter et al., 1990) and for *Scomberomorus plurilineatus* in South Africa (Chale-Matsau et al., 1999).
– SpO2: Appears to be the most common spawning origin for the fish in our study caught in Mozambique (Moz-W) (58% of narrow-barred Spanish mackerel otolith cores from Mozambique had SpO2 elemental signature). SpO2 is characterized by particularly high concentrations in Ba and Mg and may be related to the upwelling hotspot observed in Mozambique. Our hypothesis is that SpO2 may correspond to spawning grounds dominated by upwelling conditions, as can be observed in Mozambique during winter (Malauene, 2010; Vinayachandran et al., 2021a). In addition, a considerable part of narrow-barred Spanish mackerel otolith cores caught in the western Indian Ocean during winter (up to 25%) display the SpO2 elemental signatures characterized by high concentrations in Ba and Mg. This suggest that narrow-barred Spanish mackerel encountered in the western Indian Ocean may have two spawning origins following the seasonal cycle characterized by the abundance or absence of nutrients. This explanation is given some support by the fact that the otolith core chemistry analyses limited to samples from Egypt, Djibouti and Somalia also indicate two potential spawning origins.

In East Africa, these results suggesting two spawning origins are potentially driven by spawning seasonality of this species. The Indian Ocean Tuna Commission indicates that narrow-barred Spanish mackerel is characterized by two main spawning seasons, April-July and September-November

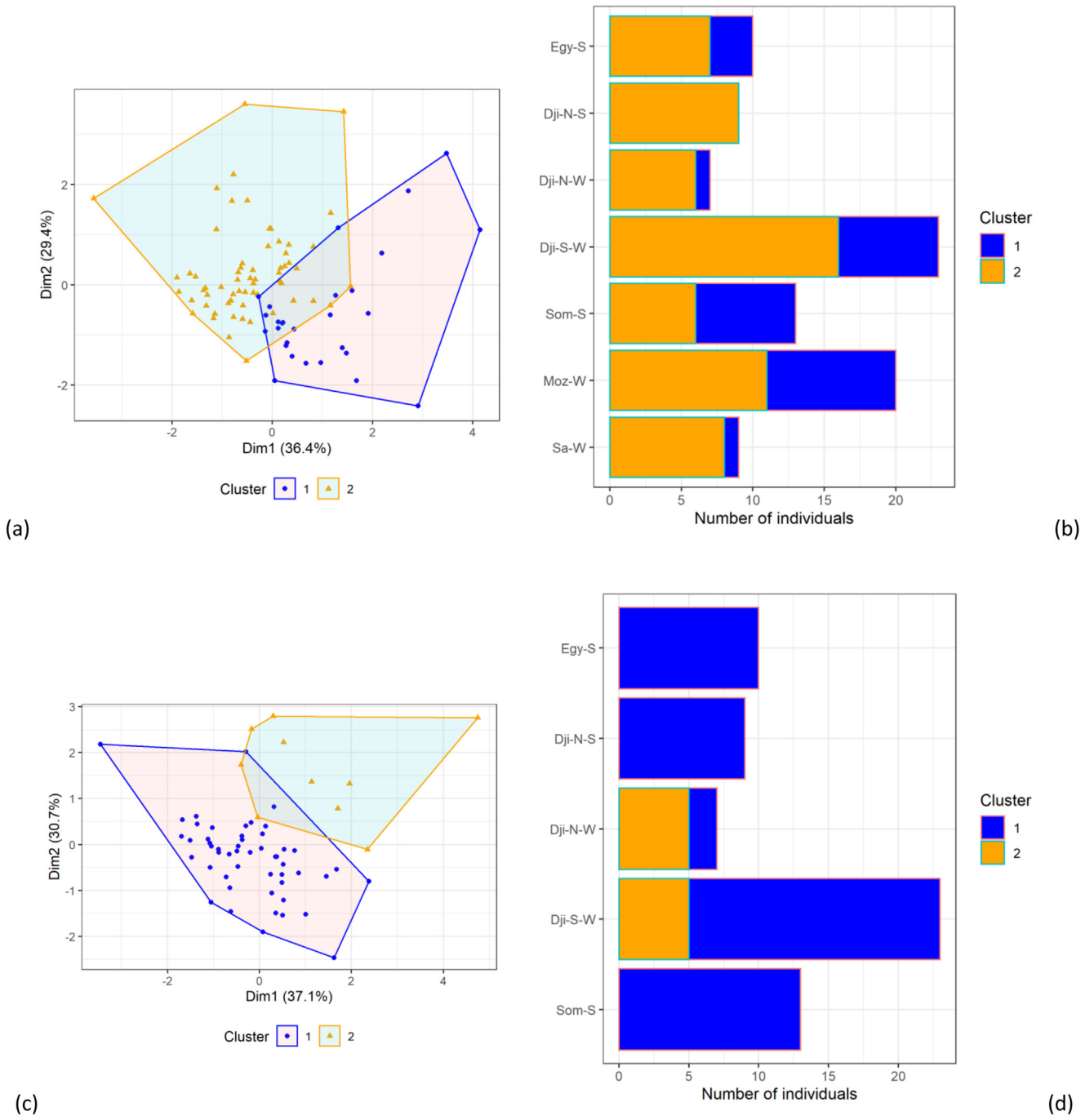

Fig. 11. Clusters obtained using agglomerative Ward's hierarchal clustering applied to the core of the otolith of all fish samples. All sampling event are represented on top row (a, b) while bottom row (c, d) includes only sampling events in Egypt, Djibouti (North and South) and Somalia and excludes samples caught in Mozambique and South Africa. Barplots on the right (b, d) indicate the number of individuals from each sampling event that were assigned to the different clusters (with (b) corresponding to the clusters in (q), and (d) corresponding to the clusters in (c)). The x-axes on the barplots represent the number of individuals for each sampling event colored by their assigned cluster.

(IOTC, 2014), though regional studies based on gonadal examinations highlight a single spawning season either in May-June (Claereboudt et al., 2005) or April-August (Grandcourt et al., 2005). It is possible that our identified two spawning origins correspond to the two main spawning seasons indicated by the IOTC in East Africa, though further research examining otolith signatures in conjunction with fine-scale otolith aging work should be carried out to confirm this.

In conclusion, the results of this study revealed the potential of the otolith chemistry approach for narrow-barred Spanish mackerel to understand the spatio-temporal dynamics of this valuable species. However, these results need to be

Table 2. Proportion (%) all sampled indiviuals from each spawning origin (SpO 1 or SpO 2) for each of the seven sampling Event in the Red Sea and the western Indian Ocean (see Tab. 1): Egypt in summer (Egy −S); North Djibouti during summer (Dji-N-S), North Djibouti during winter (Dji-N-W), South Djibouti in winter (Dji-S-W); Somalia in summer (Som-S), Mozambique in winter (Moz-W) and South Africa (Sa-W).

Spawning origin	Egy-S	Dji-N-S	Dji-N-W	Dji-S-W	Som-S	Moz-W	Sa-W
SpO-1-Cluster 1	100%	100%	71%	82%	92%	42%	89%
SpO-2-Cluster 2	0%	0%	29%	18%	8%	58%	11%

confirmed through more complete sampling (taking into account the fishing seasons for all sampling localities) and electronic tagging operations aimed at tracking large-scale movements of fish populations. Recent studies combining different techniques for delimiting stocks (microchemistry of otoliths, tagging, genetics, etc.) have shown their efficiency to enable a better understanding of the spatial dynamics for highly migratory fish species (Brophy et al., 2020; Taillebois et al., 2017). Such research will be essential to implementing regional management strategies that ensure sustainable fishing for this important exploited fish species.

Acknowledgements. This work was funded by the "Centre d'Etudes et de Recherche de Djibouti" CERD. We are grateful to Dr Mohamed Jalludin and to other colleagues in the Institute of Life Sciences (ISV) for their support and encouragement. We are also grateful to all the MARBEC research laboratory members, especially the sclerochronology and biometry technical platforms team for their help in otolith preparation. Special thanks to O. Bruguier (University of Montpellier) for his contribution to LA-ICPMS analysis and to Sean Fennessy (Oceanographic Research Institute, Durban, South Africa) for his invaluable help in collecting and sending otolith samples from Mozambique and South Africa. We sincerely thank Bruce Mann of the Oceanographic Research Institute, Durban, South Africa for providing the otolith samples from South Africa and Mozambique used in this study. We also thank the handling editor and two anonymous reviewers for their constructive comments that significantly improved the quality of the article.

Supplementary Material

The Supplementary Material is available at https://www.alr.org/10.1051/alr/2023015/olm.

References

Artetxe-Arrate I, Fraile I, Crook DA, Zudaire I, Arrizabalaga H, Greig A, Murua H. 2019. Otolith microchemistry: a useful tool for investigating stock structure of yellowfin tuna (*Thunnus albacares*) in the Indian Ocean. *Mar Freshw Res* 70: 1708–1721.

Artetxe-Arrate I, Fraile I, Farley J, Darnaude AM, Clear N, Rodríguez-Ezpeleta N, Dettman DL, Pécheyran C, Krug I, Médieu A, Ahusan M, Proctor C, Priatna A, Lestari P, Davies C, Marsac F, Murua H. 2021. Otolith chemical fingerprints of skipjack tuna (*Katsuwonus pelamis*) in the Indian Ocean: First insights into stock structure delineation. *PLOS ONE* 16: 1–18.

Bae SE, Kim J-K. 2020. Otolith microchemistry reveals the migration patterns of the flathead grey mullet Mugil cephalus (*Pisces: Mugilidae*) in Korean waters. *J Ecol Environ* 44: 21.

Brophy D, Rodríguez-Ezpeleta N, Fraile I, Arrizabalaga H. 2020. Combining genetic markers with stable isotopes in otoliths reveals complexity in the stock structure of Atlantic bluefin tuna (*Thunnus thynnus*). *Sci Rep* 10: 1–17.

Cadrin SX, Kerr LA, Mariani S. 2013. Stock identification methods: applications in fishery science. Technology & Engineering. *Academic Press*. 566 pp.

Campana S. 1999. Chemistry and composition of fish otoliths: pathways, mechanisms and applications. *Mar Ecol Prog Ser* 188: 263–297.

Chale-Matsau JR, Govender A, Beckley LE. 1999. Age and growth of the queen mackerel *Scomberomorus plurilineatus* from KwaZulu-Natal, *South Africa. Fish Res* 44: 121–127.

Charrad M, Ghazzali N, Boiteau V, Niknafs A. 2014. Determining the number of clusters using NbClust package. *Proceedings of MSDM* 2014. Available online at https://www.researchgate.net/profile/Mohamed-Limam/publication/323600098_Proceedings_of_MSDM_2014/links/5a9f7cd9aca272d448adb7cb/Proceedings-of-MSDM-2014.pdf#page=6. Accessed on 2023- 04-12.

Claereboudt MR, Mcllwain JL, Al-Oufi HS, Ambu-Ali AA. 2005. Patterns of reproduction and spawning of the kingfish (*Scomberomorus commerson*, Lacèpede) in the coastal waters of the Sultanate of Oman. *Fish Res* 73: 273–282.

Clarke AD, Telmer KH, Shrimpton JM. 2015. Movement patterns of fish revealed by otolith microchemistry: a comparison of putative migratory and resident species. *Environ Biol Fishes* 98: 1583–1597.

Collette BB. 2001. Scombridae, in: *The Living Marine Resources of the Western Central Pacific*, edited by K.E. *Carpenter and V. Niem*, pp. 3721–3756.

Collette BB, Russo JL. 1984. Morphology, systematics, and biology of the Spanish mackerels (*Scomberomorus, Scombridae*). *Wash. DC Serv.* 82: 545–692.

Devaraj M. 1983. Maturity, spawning and fecundity of the king seer, *Scomberomorus commerson* (Lacepède), in the seas around the Indian peninsula. *Indian J Fish* 30: 203–230.

Elsdon TS, Wells BK, Campana SE, Gillanders BM, Jones CM, Limburg KE, Secor DH, Thorrold SR, Walther BD. 2008. Otolith chemistry to describe movements and life-history parameters of fishes: hypotheses, assumptions, limitations and inferences. *In: Oceanography and Marine Biology*, Volume 46. CRC Press. 34 pp.

Farias I, Pérez-Mayol S, Vieira S, Oliveira PB, Figueiredo I, Morales-Nin B. 2022. Ontogenetic spatial dynamics of the deep-sea teleost Aphanopus carbo in the NE Atlantic according to otolith geochemistry. *Deep Sea Res Part Oceanogr Res Pap* 186: 103820.

Fauvelot C, Borsa P. 2011. Patterns of genetic isolation in a widely distributed pelagic fish, the narrow-barred Spanish mackerel (*Scomberomorus commerson*). *Biol J Linn Soc* 104: 886–902.

Fersi W. 2016. Reconstitution de la variabilité de la mousson indienne et ses impacts environnementaux sur le Nord-Ouest de la Mer d'Arabie et ses bordures continentales depuis le Dernier Maximum GlaciaireW étude multi-proxy d'une carotte marine dans le Golfe d'Aden (These de doctorat). *Université Paris-Saclay (ComUE)*.

Fu D. 2020. Assessment of Indian Ocean narrow-barred Spanish mackerel (*Scomberomorus commerson*) using data-limited methods | IOTC (No. IOTC-2020-WPNT10-14). *Kenya, IOTC Working Party on Neritic Tunas (WPNT)*.

Gittings JA, Raitsos DE, Racault M-F., Brewin RJW, Pradhan Y, Sathyendranath S, Platt T. 2017. Seasonal phytoplankton blooms in the Gulf of Aden revealed by remote sensing. *Remote Sens Environ* 189: 56–66.

Govender A, Al-Oufi H, McIlwain JL, Claereboudt MC. 2006. A per-recruit assessment of the kingfish (*Scomberomorus commerson*) resource of Oman with an evaluation of the effectiveness of some management regulations. *Fish Res* 77: 239–247.

Grandcourt EM. 2013. A review of the fisheries, biology, status and management of the narrow-barred Spanish mackerel (*Scomberomorus commerson*) in the Gulf Cooperation Council countries (Bahrain, Kuwait, Oman, Qatar, Saudi Arabia and the United Arab Emirates) (No. IOTC-2013-WPNT03-27). *Bali, Indonesia, IOTC Working Party on Neritic Tunas (WPNT)*.

Grandcourt EM, Al Abdessalaam TZ, Francis F, Al Shamsi AT. 2005. Preliminary assessment of the biology and fishery for the narrow-barred Spanish mackerel, *Scomberomorus commerson* (Lacépède, 1800), in the southern Arabian Gulf.*Fish Res* 76: 277–290.

Hampton SL, Moloney CL, van der Lingen CD,Labonne M. 2018. Spatial and temporal variability in otolith elemental signatures of juvenile sardine off South Africa. *J Mar Syst* 188: 109–116.

Hoolihan JP, Anandh P, van Herwerden L. 2006. Mitochondrial DNA analyses of narrow-barred Spanish mackerel (*Scomberomorus commerson*) suggest a single genetic stock in the ROPME sea area (Arabian Gulf, Gulf of Oman, and Arabian Sea). *ICES J Mar Sci* 1066–1074.

Hüssy K, Limburg KE, de Pontual H, Thomas O.R, Cook PK, Heimbrand Y, Blass M, Sturrock AM. 2020. Trace element patterns in otoliths: the role of biomineralization. *Rev Fish Sci Aquac* 29: 445–477.

IOTC. 2014. Status of the Indian Ocean narrow-barred Spanish mackerel (*Scomberomorus commerson*) resource (No. IOTC-2014-SC17-ES11). *Seychelles, Indian Ocean Tuna Commission Scientific Committee (SC)*. Available at https://iotc.org/sites/default/files/documents/2014/11/IOTC-2014-SC17-ES11E_-_Narrow-barred_Spanish_mackerel.pdf, Accessed on 2023- 04-12.

IOTC. 2017. Assessment of Indian Ocean narrow-barred Spanish mackerel (*Scomberomorus commerson*) using data limited catch-based methods (No. IOTC-2017-WPNT 07-17 Rev_1). *IOTC Working Party on Neritic Tunas (WPNT)*. Avaiable at https://iotc.org/sites/default/files/documents/2017/07/IOTC-2017-WPNT07-17_Rev_1_-_SA_COM.pdf, Accessed on 2023- 04-12.

IOTC. 2018. Status of the Indian Ocean narrow-barred Spanish mackerel (*Scomberomorus commerson*) resource (No. IOTC-2018-SC21-ES11). *Seychelles, Indian Ocean Tuna Commission Scientific Committee (SC)*. Available at https://iotc.org/sites/default/files/documents/2018/11/Narrow-barred_Spanish_mackerel_0.docx, Accessed on 2023- 04-12.

Izzo C, Reis-Santos P, Gillanders BM. 2018. Otolith chemistry does not just reflect environmental conditions: a meta-analytic evaluation. *Fish Fisheries* 19: 441–454.

Jaswal AK, Singh V, Bhambak SR. 2012. Relationship between sea surface temperature and surface air temperature over Arabian Sea, Bay of Bengal and Indian Ocean. *J Ind Geophys Union* 16: 41–53.

Kai TE, Marsac F. 2010. Influence of mesoscale eddies on spatial structuring of top predators' communities in the Mozambique Channel. *Progr Oceanogr* 86: 214–223.

Kassambara A. 2017. Practical guide to principal component methods in R: PCA, M (CA), FAMD, MFA, HCPC, factoextra. *Sthda*. 169 pp.

Kassambara A, Mundt F. 2017. Package 'factoextra.' Extr. *Vis. Results Multivar. Data Anal* 76.

Kaymaram G, Vahabnezhad D. 2013. Growth, mortality and exploitation rate of narrow-barred Spanish mackerel, *Scomberomorus commerson* in the Persian Gulf and Oman Sea, Iran, Hormozgan's waters (No. IOTC-2013-WPNT 03-29 Rev_1). *Bali, Indonesia, IOTC Working Party on Neritic Tunas (WPNT)*. Available at https://iotc.org/sites/default/files/documents/2013/06/IOTC-2013-WPNT03-29%20Rev_1%20-%20I.R.%20Iran%20Spanish%20mackerel_0.pdf, Accessed on 2023- 04-12.

Kerr LA, Campana SE. 2014. Chemical composition of fish hard parts as a natural marker of fish stocks. *In: Stock Identification Methods. Elsevier*, pp. 205–234.

Kingsford MJ, Hughes JM, Patterson HM. 2009. Otolith chemistry of the non-dispersing reef fish *Acanthochromis polyacanthus*: cross-shelf patterns from the central Great Barrier Reef. *Mar Ecol Progr Ser* 377: 279–288.

Kitchens LL, Rooker JR, Reynal L, Falterman BJ, Saillant E, Murua H. 2018. Discriminating among yellowfin tuna *Thunnus albacares* nursery areas in the Atlantic Ocean using otolith chemistry. *Mar Ecol Prog Ser* 603: 201–213.

Lê S, Josse J, Husson F. 2008. FactoMineR: an R package for multivariate analysis. *J Stat Softw* 25: 1–18.

Lee B, Mann BQ. 2017. Age and growth of narrow-barred Spanish mackerel *Scomberomorus commerson* inthe coastal waters of southern Mozambique and KwaZulu-Natal, South Africa. *Afr J Mar Sci* 39: 397–407.

Legendre P, Anderson MJ. 1999. Distance-based redundancy analysis: testing multispecies responses in multifactorial ecological experiments. *Ecol Monogr* 69: 1–24.

Lin Y-T., Wang C-H., You C-F., Tzeng W-N. 2013. Ba/ Ca ratios in otoliths of southern bluefin tuna (*Thunnus maccoyii*) as a biological tracer of upwelling in the Great Australian Bight. *J Mar Sci Technol* 21: 733–741.

Longhurst AR. 2007. The Indian Ocean. In Ecological Geography of the Sea. *San Diego, CA: Academic Press*, 2nd ed. pp. 275–320.

Malauene B. 2010. Shelf edge upwelling off northern Mozambique (Master's thesis). *Mozambique, Faculty of Science, Departments of Zoology and Oceanography University of Cape Town*.

Murtagh F, Contreras P. 2017. Algorithms for hierarchical clustering: an overview, II. *Wiley Interdiscip Rev Data Min Knowl Discov* 7: 1–20.

Murtagh F, Legendre P. 2014. Ward's hierarchical agglomerative clustering method: which algorithms implement Ward's criterion? *J Classif* 31: 274–295.

Nandkeolyar N, Raman M, Kiran GS. 2013. Comparative analysis of sea surface temperature pattern in the eastern and western gulfs of Arabian Sea and the Red Sea in recent past using satellite data. *Int J Oceanogr* 2013: 1–16.

Panfili J, Pontual H de, Troadec H, Wright P. J. (Eds.). 2018. Manuel de sclérochronologie des poissons, Manuel de sclérochronologie des poissons, Hors collection. *Marseille: IRD Éditions*. 463 pp.

Papadopoulou C, Kanias GD, Moraitopoulou-kassimati E. 1980. Trace element content in fish otoliths in relation to age and size. *Mar Pollut Bull* 11: 68–72.

Perrion MA, Kaemingk MA, Koupal KD, Schoenebeck CW, Bickford NA. 2020. Use of otolith chemistry to assess recruitment and habitat use of a white bass fishery in a Nebraska reservoir. *Lake Reserv Manag* 36: 64–74.

Quartly G, Srokosz M. 2004. Eddies in the southern Mozambique Channel. *Deep-sea Research – II. Top Stud Oceanogr* 51: 69–83.

R Core Team. 2018. A language and environment for statistical computing. *Vienna, Austria: R Foundation for Statistical Computing*.

Radigan WJ, Carlson AK, Kientz JI, Chipps SR, Fincel MJ, Graeb BD. 2018. Species- and habitat-specific otolith chemistry patterns inform riverine fisheries management. *River Res Appl* 34: 279–287.

Reygondeau G, Longhurst AR, Martinez E, Beaugrand G, Antoine D. 2013. Dynamic biogeochemical provinces in the global ocean. *Glob Biogeochem Cycles* 27: 1046–1058.

Rogers TA, Fowler AJ, Steer MA, Gillanders BM. 2019. Discriminating natal source populations of a temperate marine fish using larval otolith chemistry. *Front Mar Sci* 6: 711.

Rooker JR, David Wells RJ, Itano DG, Thorrold SR, Lee JM. 2016. Natal origin and population connectivity of bigeye and yellowfin tuna in the Pacific Ocean. *Fish Oceanogr* 25: 277–291.

Schott FA, Xie SP, McCreary Jr JP. 2009. Indian Ocean circulation and climate variability. *Rev Geophys* 47: RG1002.

Shaklee JB, Phelps SR, Salini JP. 1990. Analysis of fish stock structure and mixed-stock fisheries by the electrophoretic characterization of allelic isozymes. In: Whitmore DH (Ed.). Electrophoretic and Isoelectric Focusing Techniques in Fisheries Management. CRC Press Inc. pp. 173–196.

Sirot C, Ferraton F, Panfili J, Childs AR, Guilhaumon F, Darnaude AM. 2017. elementr: An R package for reducing elemental data from LA-ICPMS analysis of biological calcified structures. *Methods Ecol Evol* 8: 1659–1667.

Smit AJ, Roberts M, Anderson RJ, Dufois F, Dudley SF, Bornman TG, Olbers J, Bolton JJ. 2013. A coastal seawater temperature dataset for biogeographical studies: large biases between in situ and remotely-sensed data sets around the coast of South Africa. *PLoS ONE* 8: e81944.

Sofianos SS, Johns WE. 2007. Observations of the summer Red Sea circulation. *J Geophys Res* 112: C06025.

Strnad L, Ettler V, Mihaljevic M, Hladil J, Chrastny V. 2009. Determination of trace elements in calcite using solution and laser ablation ICP-MS: Calibration to NIST SRM glass and USGS MACS carbonate, and application to real landfill calcite. *Geostand Geoanaly Res* 33: 347–355.

Sturrock AM, Hunter E, Milton JA, Johnson RC, Waring CP, Trueman CN. 2015. Quantifying physiological influences on otolith microchemistry. *Methods Ecol Evol* 6: 806–816.

Sturrock AM, Trueman CN, Darnaude AM, Hunter E. 2012. Can otolith elemental chemistry retrospectively track migrations in fully marine fishes? *J Fish Biol* 81: 766–795.

Sutter FCI, Williams RO, Godcharles M. 1990. Movement patterns and stock affinities of king mackerel in the southern United States. *Fish Bull U.S.* 89: 315–324.

Taillebois L, Barton DP, Crook DA, Saunders T, Taylor J, Hearnden M, Saunders RJ, Newman SJ, Travers MJ, Welch DJ. 2017. Strong population structure deduced from genetics, otolith chemistry and parasite abundances explains vulnerability to localized fishery collapse in a large Sciaenid fish, *Protonibea diacanthus*. *Evol Appl* 10: 978–993.

Tanner SE, Reis-Santos P, Cabral HN. 2016. Otolith chemistry in stock delineation: a brief overview, current challenges and future prospects. *Fish Res* 173: 206–213.

Thorisson K, Jónsdóttir I, Marteinsdottir G, Campana S. 2011. The use of otolith chemistry to determine the juvenile source of spawning cod in Icelandic waters. *ICES J Mar Sci* 68: 98–106.

Thresher RE. 1999. Elemental composition of otoliths as a stock delineator in fishes. *Fish Res* 43: 165–204.

Van Herwerden L, McIlwain J, Al-Oufi H, Al-Amry W, Reyes A. 2006. Development and application of microsatellite markers for *Scomberomorus commerson* (Perciformes; Teleostei) to a population genetic study of Arabian Peninsula stocks. *Fish Res* 79: 258–266.

Vinayachandran PNM, Masumoto Y, Roberts MJ, Huggett JA, Halo I, Chatterjee A, Amol P, Gupta GVM, Singh A, Mukherjee A, Prakash S, Beckley LE, Raes EJ, Hood R. 2021. Reviews and syntheses: physical and biogeochemical processes associated with upwelling in the Indian Ocean. *Biogeosciences* 18: 5967–6029.

Walsh CT, Gillanders BM. 2018. Extrinsic factors affecting otolith chemistry – implications for interpreting migration patterns in a diadromous fish. *Environ Biol Fish* 101: 905–916.

Wang C-H., Lin YT, Shiao JC, You C-F., Tzeng W-N. 2009. Spatio-temporal variation in the elemental compositions of otoliths of southern bluefin tuna *Thunnus maccoyii* in the Indian Ocean and its ecological implication. *J Fish Biol* 75: 1173–1193.

Welsh DJ, Hoyle SD, McPherson G.R., Gribble NA. 2002. Preliminary assessment of the Queensland east coast Spanish mackerel fishery. *Information Series QI02110, Queensland Government, Department of Primary Industries, Cairs*.

Wheeler SG, Russell AD, Fehrenbacher JS, Morgan SG. 2016. Evaluating chemical signatures in a coastal upwelling region to reconstruct water mass associations of settlement-stage rockfishes. *Mar Eco Progr Ser* 550: 191–206.

Woodson LE, Wells BK, Grimes CB, Franks RP, Santora JA, Carr MH. 2013. Water and otolith chemistry identify exposure of juvenile rockfish to upwelled waters in an open coastal system. *Mar Ecol Progr Ser* 473: 261–273.

Yao F, Hoteit I, Pratt LJ, Bower AS, Zhai P, Köhl A, Gopalakrishnan G. 2014. Seasonal overturning circulation in the Red Sea: 1. *Model validation and summer circulation. J Geophys Res Oceans* 119: 2238–2262.

Zubier K. 2010. Sea level variations at Jeddah, eastern coast of the red sea. *J. King Abdulaziz Univ-Mar Sci* 21: 73–86.

Cite this article as:Sougueh MA, Labonne M, Daher A, Ali A, Kaplan DM. 2023. Spatiotemporal structure of narrow-barred Spanish mackerel (*Scomberomorus commerson*) from the Red Sea and western Indian Ocean based on otolith micro-chemistry. *Aquat. Living Resour.* 36: 20